Surface Review and Letters, Vol. 10, No. 4 (2003) 641–648

World Scientific
www.worldscientific.com

INITIAL GROWTH OF Co ON Cu{001} STUDIED WITH LEED I(V)

J. SAINIO,*‡§ E. ALSHAMAILEH,†‡ J. LAHTINEN* and C. J. BARNES‡¶
*Laboratory of Physics, Helsinki University of Technology,
PO Box 1100, 02015 HUT, Finland
†Plasma Research Laboratory, NCPST, School of Physical Sciences,
Dublin City University, Dublin 9, Ireland
‡School of Chemical Sciences, Dublin City University, Dublin 9, Ireland
§Jani.Sainio@hut.fi

Received 10 October 2002

The initial growth of Co deposited at room temperature on Cu{001} was studied with low energy electron diffraction (LEED) and temperature-programmed desorption (TPD). Measured I(V) spectra were compared with calculated spectra from several model structures, including substitutionally disordered alloys. The averaged T-matrix approximation (ATA) was used to model the random alloy layers. According to the I(V) analysis, alloying occurs in the first stages of the growth. TPD of CO indicates that both large areas of Co and areas of a surface alloy are already present at the lowest coverage. Both methods show that a transition to layer-by-layer growth occurs as the coverage increases.

Keywords: Low energy electron diffraction; cobalt; copper; single crystal epitaxy; temperature-programmed desorption.

1. Introduction

Ultrathin films of ferromagnetic materials on non-magnetic substrates have recently been the subject of many studies because of their interesting magnetic properties, like giant magnetoresistance[1] and magnetic anisotropy.[2] Especially, pseudomorphic growth of Fe and Co on Cu{001} has been the object of many investigations.[3–6] Layer-by-layer growth has been reported for Co on Cu{001}.[7,8] However, the growth mode at low coverages deviates from the layer growth and depends strongly on the growth rate.[9] The substrate temperature plays an important role also, since significant Cu surface segregation has been found at temperatures over 400 K.[3] This process should also occur at room temperature, but on a longer time scale.

The structure and the quality of the films affect the magnetic properties of the interface system. In order to understand the magnetic properties of the system it is important to determine the structure of these ultrathin films. Recently, STM studies at room temperature have shown Co atoms incorporated into the first substrate layer.[9,10] A c(2×2) surface alloy was reported to form at slightly elevated temperatures.[11] STM is an excellent method for surface studies, but it cannot directly distinguish between cobalt and copper atoms and it gives no information on the underlying structure.

There have been several LEED I(V) studies on the Cu{001} substrate,[12–17] including ones with Co, but the possibility of alloying during initial growth has not been considered. In this work LEED I(V)

§Corresponding author. Tel.: +358 9 451 3130. Fax: +358 9 451 3116.
¶Passed away in May 2002.

structural determination and thermal desorption spectroscopy were used to study the growth. In addition to layer-by-layer growth, subsurface layers and substitutionally disordered alloys were considered in the LEED I(V) calculations. The disorder was taken into account with the averaged T-matrix approximation (ATA).[18–22] Thermal desorption spectra of CO were measured for all studied coverages to probe Co atoms on the surface.

2. Experimental

Experiments were carried out in an ultrahigh vacuum chamber with a base pressure of $2 \cdot 10^{-10}$ Torr. The chamber had facilities for LEED, Auger spectroscopy and thermal desorption spectroscopy. The standard sample cleaning procedure involved sputtering for 30 min with 3 keV Ar^+ ions followed by annealing at 650 K for 10 min. The cleanliness of the sample was checked by observing the quality of the substrate p(1 × 1) LEED pattern.

Cobalt was evaporated from a 0.125 mm high purity cobalt wire wrapped around a spiral tungsten filament. During deposition the substrate temperature was in the range of 300–320 K. The pressure during evaporation was kept under $1 \cdot 10^{-9}$ Torr.

The amount of deposited cobalt was calibrated by measuring the attenuation of the Cu 59 eV M_3VV Auger peak. If we consider only full layers, the attenuation of the substrate peak is known to be exponential:

$$\frac{I_{\mathrm{CU}}}{I^0_{\mathrm{CU}}} = e^{-\frac{x}{\lambda_{\mathrm{EAL}} \cos\theta}}, \qquad (1)$$

where x is the thickness of the film, θ the average acceptance angle of the analyzer and λ_{EAL} the effective attenuation length. Equation (1) can be modified to give the attenuation for structures with alloy layers. The substrate signal for a structure with n alloy layers of equal thickness d will be

$$\frac{I_{\mathrm{CU}}}{I^0_{\mathrm{CU}}} = e^{-\frac{nd}{\lambda_{\mathrm{EAL}} \cos\theta}} + \sum_{i=1}^{n} D_i (1 - e^{-\frac{d}{\lambda_{\mathrm{EAL}} \cos\theta}}) e^{-\frac{(n-1)d}{\lambda_{\mathrm{EAL}} \cos\theta}}, \qquad (2)$$

where D_i is the fraction of substrate atoms in the ith layer. This equation can be used to evaluate the attenuation of the substrate signal for surface structures with full layers.

Three coverages, corresponding to evaporation times of 6, 12 and 18 min, were chosen for the analysis based on the Auger measurements of the substrate signal. The coverages were chosen to represent effective nominal coverages of one, two and three monolayers (ML). The Auger intensity ratios for these coverages were 0.61 ± 0.05, 0.43 ± 0.05 and 0.23 ± 0.07. Equation (2) can now be used to find the structures that give the same intensity ratio within error limits. Layer-by-layer growth gives the highest attenuation of the substrate signal. The amount of deposited Co with the same substrate signal attenuation will be larger for alloys and subsurface structures.

The inelastic mean free path for 59 eV electrons in Cu is 5 Å, obtained from the NIST Database.[23] If elastic scattering is neglected, the effective attenuation length (λ_{EAL}) will be the same as the inelastic mean free path. However, Powell *et al.*[24] have reported that the correction due to the elastic-electron scattering can change the effective attenuation length quite drastically. From Monte Carlo simulations, an effective attenuation length of 70% of the inelastic mean free path was found for the 59 eV Auger transition of Cu.[25] This value was utilized in evaluating the attenuation. For the layer thickness, a value of 1.8 Å was used, and for the average acceptance angle a value of 20°, based on the geometry of the retarding field analyzer, was used.

The LEED I(V) curves were measured with a rear-view unit and recorded with a videocamera connected to a data acquisition system which was also used to control the LEED beam, enabling automated measurements. At all Co depositions the surface exhibited a p(1×1) LEED pattern, implying pseudomorphic growth on the substrate. Since no fractional order spots were observed, the I(V) spectra were measured from integral order beams only. Spot intensities were collected for four beams at energies between 50 and 500 eV. The measured beams were [1,0], [1,1], [2,0] and [2,1]. For each beam the intensities were collected from at least four symmetric spots and averaged together. The symmetry-averaged beams are shown in Fig. 1 for all deposition times after a linear beam current correction.

TPD spectra for CO were also measured for all the coverages used in the LEED experiments. CO does not adsorb on Cu{001} at room temperature.[26] On the other hand, the most intense desorption peak

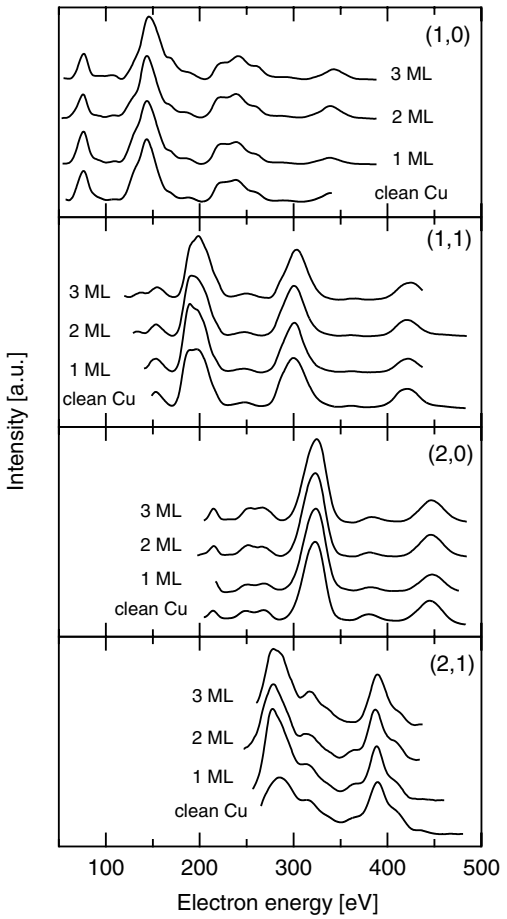

Fig. 1. Measured symmetry-averaged I(V) curves for all three effective cobalt coverages and for clean Cu{001}.

of CO on Co(0001) is around 400 K.[27] Hence, the CO TPD peak was used as a sensitive probe for the presence of surface Co.

3. Calculations

The theoretical I(V) spectra were calculated with the Symmetrized Automated Tensor LEED package of Barbieri and Van Hove.[28] The phase shifts were evaluated using the Barbieri/Van Hove phase shift package.[28] Nine phase shifts were used for Cu and Co. The real part of the inner potential was a free parameter and the imaginary part was optimized manually. The surface Debye temperatures for Cu and Co were 270 K and 360 K. Bulk values, 315 K for Cu and 385 K for Co, were used for other layers. The interlayer spacing was initially set at 1.81 Å and the in-plane atomic separation at 2.56 Å. A contraction of the in-plane separation of Cu{001} surface atoms has been reported,[29] but this has been shown to be a computational effect arising from the use of a non-energy-dependent imaginary part of the inner potential.[30] In this work the in-plane atomic separations were set at bulk values.

Theoretical and experimental spectra were compared using the Pendry R-factor.[31] The total energy range for the four integral beams was 1100 eV. The spectra were calculated for four symmetric diffraction beams which were averaged together and compared with the measured spectra. Both experimental and calculated spectra were subjected to a three-point smoothing.

If alloying is occurring in the first stages of the growth, the alloy should be a random one, since no fractional order beams were observed with LEED. The averaged T-matrix approximation (ATA) was used to model these random alloys. In this approximation, the scattering is described by an effective scattering amplitude by averaging the scattering amplitudes (t-matrices) of different scatterers together. The composition of atomic species is used as weight factors for the averaging. A more accurate method would be the coherent potential approximation (CPA), which, however, is far more complex, involving evaluation of configurational averages. The differences in the LEED I(V) analysis when using the CPA or ATA have been shown to be almost negligible,[32] justifying the use of the ATA. Four ATA layers were used in this analysis for all coverages. The Co coverage was varied in steps of 25% within each layer. Only structures giving the correct signal ratio from Eq. (2) were considered in the analysis, and only full layers were used in the I(V) analysis.

4. Results

4.1. *Error estimation in ATA*

Errors for the chemical composition in the ATA layers are usually taken from the variance of the Pendry R-factor. The errors are evaluated by finding the values that give an R-factor below the value $R_p + \mathrm{var}(R_p)$.[31] In the Co/Cu system this leads to quite large errors, because of the similar scattering properties of Co and Cu.

In a case study on the accuracy of the ATA using a clean Rh(111) surface, and mixing Pt in the first

four layers with ATA, the errors of the chemical composition evaluated from the Pendry R-factor were about 20%.[33] However, the deviation of the best-fit structure from the known composition of 100% Rh was only about 8%, showing that the true error can be smaller than the one evaluated from the Pendry R-factor variance.

A similar independent error analysis was carried out for the Co/Cu system by checking how well the averaged T-matrix approximation would perform with a clean Cu{001} surface. The I(V) spectra were calculated for different amounts of cobalt in the first four layers and compared with the I(V) spectra measured from a clean Cu{001} surface. The difference between the minima found and the known composition of 0% Co should describe the true error in the calculations. Since the minima should be at 0%, we should also allow for negative cobalt concentrations, even though this might introduce some unphysical features in the calculations. The total amount of Cu and Co was always kept at 100%.

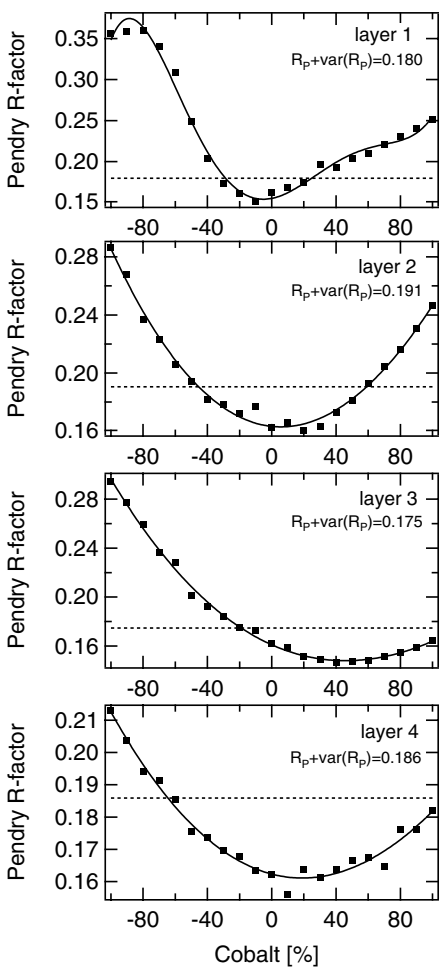

Fig. 2. The variation of the Pendry R-factor with Co concentration for the first, second, third and fourth layers in the case of the clean surface. The Pendry R-factor variance limit is also shown. The solid lines are drawn to guide the eye.

Figure 2 shows the Pendry R-factor as a function of cobalt coverage in the first four layers when comparing with the I(V) spectra from the clean surface. The variance limit $R_p + \mathrm{var}(R_p)$ is also shown. The R-factor minima for the first two layers are within 20% of the known value of 0% Co. The third layer gives the largest deviation of 40%. The variance error, however, can be as large as 80%. Based on this analysis it would seem that the true error in the chemical composition is smaller than the one given by the R-factor variance.

4.2. *Structural determination*

The structures chosen for the I(V) analysis of the 1 ML effective coverage were a cobalt overlayer, a copper-terminated cobalt bilayer and different substitutionally disordered alloy structures, in order to include all possible growth models. The structures were chosen to give the correct intensity ratio from Eq. (2) compared to the experimental value of 0.61 ± 0.05.

The resulting Pendry R-factors for the different structures are shown in Table 1. Only alloy structures with the best agreement are shown. At this stage, layer-by-layer growth can be ruled out since a Co overlayer gave an unacceptable R-factor of 0.25. Structures with a copper-rich first layer and cobalt in deeper layers gave the best agreement with the measurement. The best R-factors were given by random alloys with 25% Co in the top layer. Copper termination of the surface has been found to be energetically favorable,[34] but this sort of growth can be kinetically restricted. Metastable structures, such as bilayer alloys, have been suggested in theoretical studies.[34,35]

In the analysis of the 2 ML effective coverage, a two-layer-thick cobalt layer had to be excluded on the basis of the Auger intensity comparison. The structures accepted in the analysis were mostly ones with alloy layers. The R-factors for the best structures are shown in Table 1. Structures with a cobalt

Table 1. Pendry R-factors for selected structures from different effective coverages. The favored structures are emphasized.

Layer 1	Layer 2	Layer 3	Layer 4	Pendry R-factor
$\theta_{\text{eff}} = 1$ ML				
Co	Cu	Cu	Cu	0.25
Cu	Co	Co	Cu	0.23
$Co_{25}Cu_{75}$	$Co_{50}Cu_{50}$	$Co_{75}Cu_{25}$	Cu	0.16
$Co_{25}Cu_{75}$	$Co_{25}Cu_{75}$	Co	$Co_{25}Cu_{75}$	0.15
$\theta_{\text{eff}} = 2$ ML				
Co	Cu	Co	Co	0.26
Co	$Co_{75}Cu_{25}$	Cu	Cu	0.25
$Co_{25}Cu_{75}$	$Co_{75}Cu_{25}$	Co	$Co_{75}Cu_{25}$	0.17
$Co_{50}Cu_{50}$	$Co_{50}Cu_{50}$	Co	$Co_{25}Cu_{75}$	0.16
$\theta_{\text{eff}} = 3$ ML				
Co	Co	Co	Cu	0.20
Co	Co	Cu	Co	0.28
$Co_{75}Cu_{25}$	Co	Co	Co	0.18
$Co_{75}Cu_{25}$	Co	Co	$Co_{75}Cu_{25}$	0.18

overlayer gave again poor agreement. Hence, the top layer should consist of an alloy at this coverage. The best agreement with an R-factor of 0.16 was given by a structure with 50% Co in the first, 50% Co in the second, 100% Co in the third and 25% Co in the fourth. The measured and calculated I(V) spectra for this structure are shown in Fig. 3.

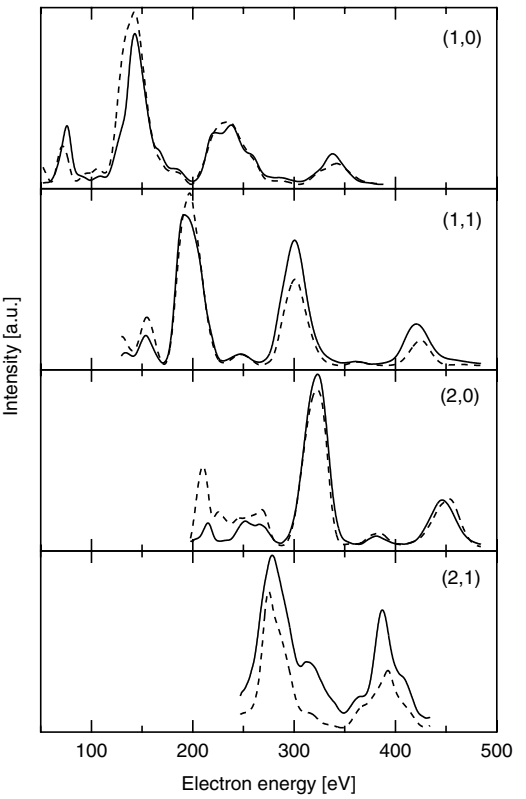

Fig. 3. Calculated I(V) curves (dotted lines) for a substitutionally disordered alloy with 50% Co in the first, 50% Co in the second, 100% Co in the third and 25% Co in the fourth layer compared to the I(V) spectra measured for the 2 ML effective Co coverage (solid lines). The Pendry R-factor is 0.16.

Structures used in the analysis of the 3 ML effective coverage included a three-layer-thick cobalt overlayer, structures with a full cobalt top layer as well as alloy terminated structures. The R-factors for these structures are shown in Table 1. A simple overlayer structure with three full cobalt layers gave a very good R-factor of 0.20. The best fit with an R-factor of 0.18 was still given by an alloy-terminated structure, although the Co coverage in the first layer was 75%.

Table 2. Best fit structures for favored compositions. The Cu{001} bulk layer spacing is 1.81 Å.

Structure	d_{xy}	Layer separation (Å)
$\theta_{\text{eff}} = 1$ ML	d_{12}	1.78 ± 0.02
$Co_{25}Cu_{75}/Co_{50}Cu_{50}/Co_{75}Cu_{25}/Cu$	d_{23}	1.82 ± 0.02
	d_{34}	1.83 ± 0.03
$\theta_{\text{eff}} = 2$ ML	d_{12}	1.80 ± 0.02
$Co_{50}Cu_{50}/Co_{50}Cu_{50}/Co/Co_{25}Cu_{75}$	d_{23}	1.81 ± 0.02
	d_{34}	1.83 ± 0.03
$\theta_{\text{eff}} = 3$ ML	d_{12}	1.78 ± 0.02
$Co_{75}Cu_{25}/Co/Co/Co_{75}Cu_{25}$	d_{23}	1.83 ± 0.02
	d_{34}	1.83 ± 0.03

The interlayer relaxations of the top four free layers were very small in all of the favored structures, which is quite reasonable considering the similar sizes of Cu and Co atoms. The interlayer spacings for some of the favored structures are given in Table 2. The errors are calculated using the Pendry R-factor variance.

The deposition times used in the experiments increased linearly and so should the Co coverage in the best fit structures. There is a deviation from this linear dependence in the obtained best fit structures. However, several alloy structures gave quite similar R-factors but different Co coverages. The chemical accuracy is better in the first and second layers than in the deeper ones, where the amount of Co can be exaggerated.

The performed LEED I(V) analysis does not give unambiguous results, but it is clear that substitutional alloy structures produce a much better data fit than overlayer structures, despite the small coverage discrepancy.

4.3. *CO TPD*

Figure 4 shows CO TPD spectra from the examined structures. The CO dosage was 20 L (1 L = 10^{-6} Torr·s) to ensure saturation coverage. The TPD spectra of the fresh films consist of two peaks with peak temperatures of about 372 K and 408 K.

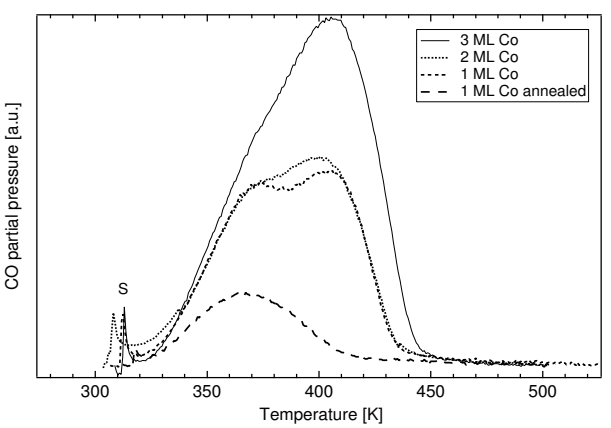

Fig. 4. CO thermal desorption spectra for the effective Co coverages used in the analysis. A TPD spectrum after Co deposition and subsequent heating past the Cu segregation temperature is also shown. The heating rate was 3.2 K/s. The sharp peaks S are due to desorption from the support wires.

Assuming first order desorption, these desorption temperatures correspond to activation energies of 1.00 and 1.10 eV/atom. The fact that the spectrum is similar for the two lower coverages suggests that the surface structure is also similar. The higher temperature peak in the TPD spectra is very similar to the clean Co(0001) 400 K peak and could therefore be attributed to CO adsorbing from larger areas of Co. This peak becomes pronounced at the highest Co coverage, supporting the assumption of growth mode change.

TPD experiments were also carried out for all three effective coverages after heating to 550 K, which is above the Cu surface segregation temperature. The desorption spectrum was essentially the same for all deposition times in both peak position and intensity. A typical TPD spectrum from these heated samples can also be seen in Fig. 4. There is only one peak visible, which is located at the same temperature as the lower temperature peak in the nonheated samples, but which has a lower intensity. This desorption feature could arise from surface Co atoms of the alloy phase. The TPD spectra would then imply that both areas of a surface alloy and areas of Co clusters exist on the surface before annealing even at the lowest coverage.

5. Discussion

The I(V) analysis gives the best agreement with effective 1 ML Co coverage for structures with a copper-rich first layer and Co deeper in the sample. Copper segregation to the surface should not occur at these temperatures; however, copper atoms released in the formation of a substitutional alloy may form islands on the surface. These copper islands may cover areas of the disordered alloys or even larger areas of Co and lead to an almost copper-covered surface even without segregation.

The higher Co coverage gives the best agreement for alloy structures as well. For the 3 ML effective coverage, structures with an almost cobalt-covered surface give good agreement, showing a shift in the growth mode toward overlayer growth. The growth mode change is also observed with TPD, where the intensity of the higher temperature feature, which can be attributed to bulklike Co, increases drastically at the highest coverage. CO thermal desorption also shows that the surface structure is similar

for the two lower coverages and that two different cobalt species exist at the surface.

Sachtler *et al.*[36] have reported that the activation energy for desorption can decrease when an alloy is formed due to the so called *ligand effect*. If CO adsorbs in the alloy phase at the on-top site of Co as it does on a Co(0001) surface,[27] it will not form bonds with Cu atoms. If the Co atoms are incorporated into the first layer, the bonds between Cu and Co atoms can affect the strength of the Co–CO bond, even without direct Cu–CO bonding. This effect has been observed, for example, on Pt/Sn alloys for CO desorption, where the CO bond strength increases with Pt concentration.[37] In a study of Pd growth on aluminum substrates two CO desorption peaks were also found and the lower temperature peak was attributed to the formation of a Pd–Al surface alloy.[38] A recent study on the electronic structure of the Co/Cu{001} system has shown that the Co 3*d* bands are not bulklike in the first stages of the growth, but that a continuous transition to a bulklike state occurs.[39] This dependency of the electronic structure of Co on coverage could well be observed in CO adsorption.

The CO desorption experiments carried out on an annealed surface show only the lower temperature peak with reduced intensity. Since the surface should be copper-terminated after annealing, it seems reasonable to assume that the remaining surface cobalt atoms are incorporated in the top layer. In this light we suggest that the lower temperature peak in fact corresponds to desorption from a surface alloy species. TPD does not give direct information on the structure of this initially formed alloy, but the LEED I(V) analysis suggests that this alloy could extend to deeper layers than just the first one.

LEED I(V) studies are a powerful tool in structure determination. The similarities in scattering properties of Cu and Co make these studies and the interpretation of the results more difficult. The sensitivity of the ATA for chemical composition is not very good and the errors if measured with the Pendry R-factor variance become quite large. However, the clean surface analysis performed in this work shows that the true error is smaller. LEED I(V) analysis together with the averaged T-matrix approximation can be used to characterize substitutionally disordered alloys even if the scattering properties of the different atomic species are similar.

6. Conclusions

LEED I(V) structural determination including the averaged T-matrix approximation and CO temperature-programmed desorption studies were used to study the initial growth of Co on Cu{001}. Both I(V) and TPD show that alloying occurs in the initial stages of Co growth, indicating also a transition to overlayer growth with increasing coverage. LEED I(V) results suggest that the initially formed random alloy is not restricted to the first layer.

Acknowledgments

This work was supported by the Academy of Finland. J. Sainio gratefully acknowledges the financial support of the Finnish Academy of Science and Letters. We also acknowledge the fruitful discussions with Prof. Matti Lindroos.

References

1. G. Binasch, P. G. F. Saurenbach and W. Zinn, *Phys. Rev.* **B39**, 4828 (1989).
2. S. van Dijken, G. D. Santo and B. Poelsema, *Phys. Rev.* **B63**, 104431 (2001).
3. M. T. Kief and W. F. Egelhoff, *Phys. Rev.* **B47**, 10785 (1993).
4. C. M. Schneider, P. Bressler, P. Schuster, J. Kirschner, J. J. de Miguel and R. Miranda, *Phys. Rev. Lett.* **64**, 1059 (1990).
5. N. Levanov, V. S. Stepanyuk, W. Hergert, O. S. Trushin and K. Kokko, *Surf. Sci.* **400**, 54 (1998).
6. J. Fassbender, U. May, B. Schirmer, R. M. Jingbut, B. Hillebrands and G. Güntherodt, *Phys. Rev. Lett.* **75**, 4476 (1995).
7. L. Gonzalez, R. Miranda, M. Salmarón, J. A. Vergés and F. Ynduráin, *Phys. Rev.* **B24**, 3245 (1981).
8. H. Li and B. P. Tonner, *Phys. Rev.* **B40**, 10241 (1989).
9. J. Fassbender, A. Allespach and U. Dürig, *Surf. Sci. Lett.* **383**, L742 (1997).
10. F. Nouvertné, U. May, M. Banning, A. Rampe, U. Korte, G. Güntherodt, R. Pentcheva and M. Scheffler, *Phys. Rev.* **B60**, 14382 (1999).
11. F. Nouvertné, U. May, A. Rampe, M. Gruyters, U. Korte, R. Brendt and G. Güntherodt, *Surf. Sci.* **436**, L653 (1999).
12. A. Clarke, G. Jennings, R. F. Willis, P. J. Rous and J. B. Pendry, *Surf. Sci.* **187**, 327 (1987).
13. J. R. Cerdá, P. L. de Andres, A. Cebollada, R. Miranda, E. Navas, P. Schuster, C. M. Schneider and J. Kirschner, *J. Phys.: Condens. Matter* **5**, 2055 (1993).

14. E. AlShamaileh and C. J. Barnes, *Phys. Chem. Chem. Phys.* **4**, 5148 (2002).
15. E. AlShamaileh, H. Younis, C. J. Barnes, K. Pussi and M. Lindroos, *Surf. Sci.* **515**, 94 (2002).
16. A. Mikkelsen and D. L. Adams, *Phys. Rev.* **B60**, 2040 (1998).
17. S. H. Kim, K. S. Lee, H. G. Min, J. Seo, S. C. Hong, T. H. Rho and J.-S. Kim, *Phys. Rev.* **B55**, 7904 (1997).
18. R. Döll, M. Kottcke and K. Heinz, *Phys. Rev.* **B48**, 1973 (1993).
19. S. K. Lee, J. S. Kim, Y. Cha, W. K. Han, H. G. Min, J. Seo and S. C. Hong, *Phys. Rev.* **B65**, 14423 (2002).
20. Y. Gauthier, Y. Joly, Baudoing and J. Rundgren, *Phys. Rev.* **B31**, 6216 (1985).
21. F. Jona, K. O. Legg, H. D. Shih, D. W. Jepsen and P. M. Marcus, *Phys. Rev. Lett.* **40**, 1466 (1978).
22. Y. Gauthier, R. Baudoing, J. Rundgren and M. Lundgren, *Phys. Rev.* **B35**, 7867 (1987).
23. C. Powell and A. Jablonski, NIST Inelastic-Mean-Free-Path Database — Version 1.0 (National Institute of Standards and Technology, Gaithersburg MD, 1999).
24. C. Powell, A. Jablonski, I. S. Tilinin, S. Tanuma and D. R. Penn, *J. Electron Spectrosc. Relat. Phen.* **98–99**, 1 (1999).
25. Z.-J. Ding and R. Shimizu, *Surf. Interf. Anal.* **23**, 351 (1999).
26. C. F. McConville, D. P. Woodruff, K. C. Prince, G. Paolucci, V. Chab, M. Surman and A. M. Bradshaw, *Surf. Sci.* **116**, 221 (1986).
27. J. Lahtinen, J. Vaari and K. Kauraala, *Surf. Sci.* **418**, 502 (1998).
28. A. Barbieri and M. A. Van Hove, http//:electron.lbl.gov/software (2001).
29. S. Müller, A. Kinne, M. Kottcke, R. Metzler, P. Bayer, L. Hammer and K. Heinz, *Phys. Rev. Lett.* **75**, 2859 (1995).
30. S. Walter, V. Blum, L. Hammer, S. Müller, K. Heinz and M. Giesen, *Surf. Sci.* **458**, 155 (2000).
31. J. B. Pendry, *J. Phys. Rev.* **C13**, 93 (1980).
32. L. Schwartz, F. Brouers, A. V. Vedyayev and H. Ehrenreich, *Phys. Rev.* **B4**, 3383 (1971).
33. M. Sporn, E. Plazgummer, S. Forsthuber, M. Schimd, W. Hofer and P. Varga, *Surf. Sci.* **416**, 423 (1998).
34. N. A. Levanov, V. S. Stepanyuk, W. Hergert, D. I. Bazhanov, P. H. Dederichs, A. Katsnelson and C. Massobrio, *Phys. Rev.* **B61**, 2230 (2000).
35. R. Pentcheva and M. Sheffler, *Phys. Rev.* **B61**, 2211 (2001).
36. W. M. H. Sachtler and R. A. V. Santen, *Advan. Catal.* **26**, 69 (1997).
37. H. Verbeek and W. M. H. Sachtler, *J. Catal.* **42**, 257 (1976).
38. V. Matolin, I. Stará, N. Tsud and V. Johánek, *Prog. Surf. Sci.* **67**, 167 (2001).
39. C. Pampuch, O. Rader, R. Kläsges and C. Carbone, *Phys. Rev.* **B63**, 153409 (2001).